Transactions of the Korean Nuclear Society Autumn Meeting
Changwon, Korea, October 20-21, 2022

Thermal Analysis of the CANDU Spent Fuel Storage Silo

Tae Gang Lee [a], Jae Jun Jeong [a*], Yong Deog Kim[b], Tae Hyeon Kim[b], Tae Hyung Na[b].
[a]*School of Mechanical Engineering, Pusan National University (PNU)*
[b]*Central Research Institute, Korea Hydro & Nuclear Power Co., Ltd*
[*]*Corresponding author: jjjeong@pusan.ac.kr*

1. Introduction

The CANDU spent fuel storage silo (the silo facility) is dry interim storage facility of spent nuclear fuel from CANDU-type reactors. The silo facility consists of four main components. The first is the concrete silo in Fig.1-(a), the second is the carbon steel liner in Fig.1-(b), the third is the stainless-steel storage basket in Fig.2, and the last is nuclear fuel rod bundles in Fig.3. Nine baskets are stored in the silo, and 60 fuel rod bundles are stored in one basket. Silo is designed to shield the radioactivity of spent fuel for 50 years and passively remove decay heat.

The purpose of an interim storage facility is to temporarily store spent nuclear fuel until a decision is made regarding the final disposal. However, as the decision about final disposal was delayed, there were many cases in which the interim storage period was extended beyond the design period. To approve the extension of the interim storage period, it is necessary to accurately identify the thermal characteristics of the facility and prove the integrity for the extended period. Therefore, a more realistic thermal analysis is needed instead of the previous conservative thermal analysis [1].

The object of this study is to evaluate the thermal characteristics of the silo facility more realistically and efficiently than before. To achieve that, finite element analysis using ANSYS FLUENT 2021 R2, a commercial CFD code, was applied.

Before analyzing the thermal characteristics of the silo facility, the thermal characteristics inside the storage basket were evaluated. At present, there is only one experiment related to the storage basket, "Storage Basket Heat Transfer Assessment of the MAXSTOR /KN-400 Storage Module, Whiteshell Lab [2]". Therefore, it is difficult to prove the validity of the thermal analysis. To overcome this, CFD analysis of the above experiment was performed, and the results were used for thermal analysis of the silo facility.

After that, a two-step scheme was established for thermal analysis of the silo facility for computational efficiency. A total of 2,220 fuel rods are stored in one basket, and 19,800 fuel rods are stored in one silo. It is very inefficient to analyze all these fuel rods explicitly. Therefore, it is necessary to reasonably simplify the geometry of the basket prior to thermal analysis of the entire facility. For reasonable simplification, the effective thermal conductivity (ETC), proposed in "Spent Nuclear Fuel Effective Thermal Conductivity Report [3]", was used. The ETC is a virtual thermal conductivity applied to predict peak cladding temperature (PCT) in a homogeneous heating solid in place of a fuel assembly. And in the first step, the correlation of the ETC was derived. After that, in the second step, thermal analysis was performed on the silo facility to which a simplified basket was applied. Boundary conditions for thermal analysis were set conservatively. And the thermal analysis results were compared with the design criteria for the facility.

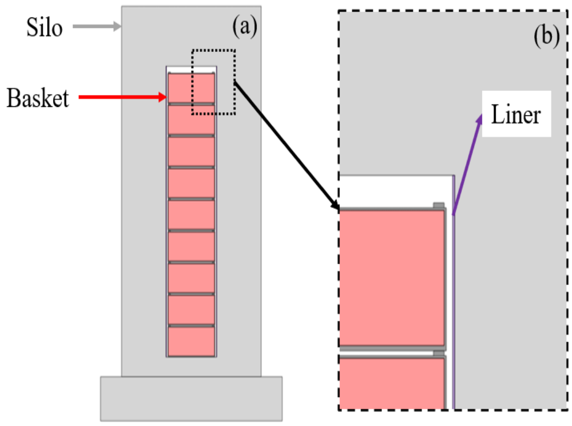

Fig.1. The schematic of the concrete silo.

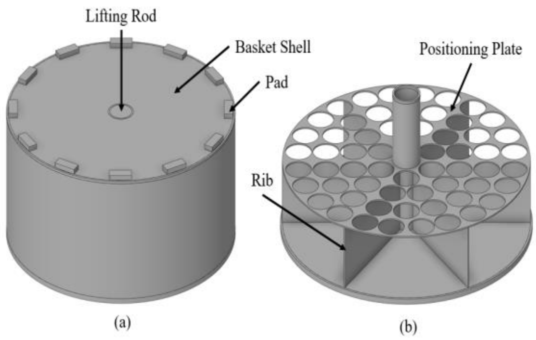

Fig.2. Fuel bundle storage basket.

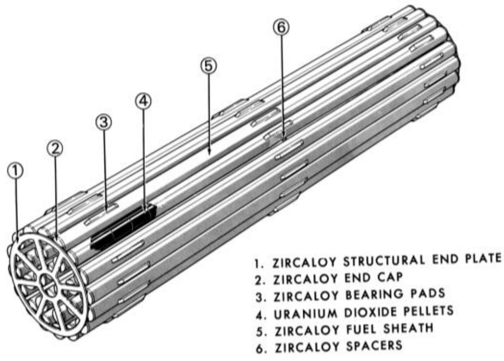

Fig.3. The CANDU-37 fuel bundle.

2. Evaluating Thermal Characteristics of the Storage Basket

The CFD analysis was performed on the thermal experiment for the storage basket conducted by Whiteshell Lab. However, since the experiment was conducted using mock-up cylinders instead of fuel rod bundles, the analysis results cannot be directly used for the thermal analysis for the silo facility. Therefore, CFD analysis focused on identifying the qualitative thermal characteristics inside the basket.

2.1 The Experiment Overview

A heat transfer assessment experiment for the storage basket was conducted by the Whiteshell Lab under AECL in Canada. In the experiment, the 6watt output mock-up cylinder (Fig.4-(a)) was used instead of the CANDU-37 type nuclear fuel rod bundle. As shown in the Fig.4-(b), the upper and lower ends of the basket are insulated, and 60 cylinders are stored in the basket.

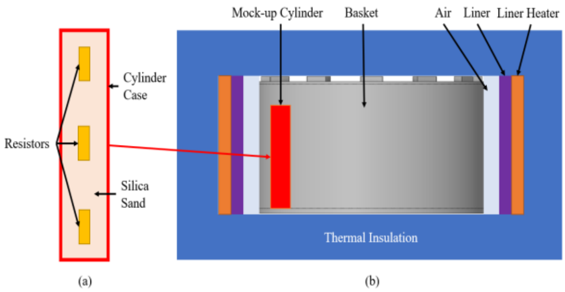

Fig.4. The schematics of the mock-up cylinder and the experiment.

Steady-state results were obtained when the temperature of the liner surrounding the basket was 96°C by actuating the electrical resistance in the cylinder. The experimental results are summarized in the Table 1.

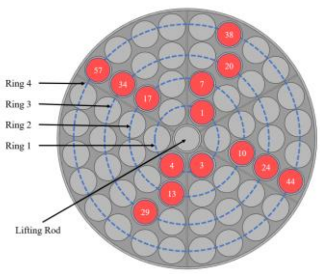

Fig.5. Cross section of the basket mock-up.

Table 1. The experiment results.

Ring Number	Cylinder Number	Measured Temperature
1	1	159.4℃
	3	159.2℃
	4	159.3℃
Average Temperature		159.2℃
2	7	154.7℃
	10	156.9℃
	13	155.0℃
	17	154.6℃
Average Temperature		155.3℃
3	20	147.7℃
	24	149.3℃
	29	148.3℃
	34	148.4℃
Average Temperature		149.1℃
4	38	137.5℃
	44	141.1℃
	57	139.4℃
Average Temperature		139.3℃
Basket Shell 1		116.7℃
Basket Shell 2		115.1℃
Basket Shell 3		113.7℃
Average Temperature		115.2℃

2.2 CFD Analysis of the Storage Basket

ANSYS SpaceClaim 2021 R2, a commercial pre-processing program, was used for geometry generation. Considering the symmetry of the basket design, an axisymmetric 1/6 basket was applied to the computational domain. In addition, the top and bottom plates of the basket were ignored, and the central lifting rod was also ignored.

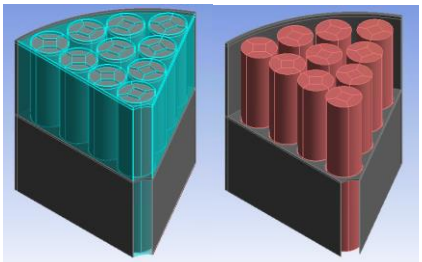

Fig.6. Basket geometry for the CFD analysis.

The mesh was created using ANSYS Mesh 2021 R2. The FLUENT solver setup was referenced in previous study [4] and NUREG-2152 [5], and is summarized in Table 2.

Table 2. FLUENT solver setup.

Viscous Model		Laminar Model
Radiation Model		DO model
Density Model		Incompressible Ideal Gas Model
Pressure – Velocity Coupling		SIMPLE
Spatial Discretization	Gradient	Least Squares Cell Based
	Pressure	Body Force Weighted
	Momentum	2nd Order Upwind
	Energy	2nd Order Upwind
	DO	2nd Order Upwind

Boundary conditions for the CFD analysis were set as shown in the Fig.7, and the experimental results were referred to for heat source per basket (360W) and wall isothermal conditions (115.2℃).

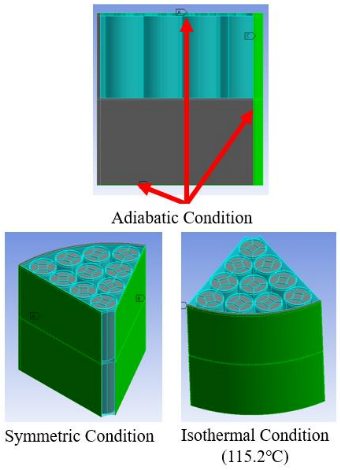

Fig.7. Boundary conditions for the CFD Analysis.

The mesh independence study results are summarized in Table 3, and the mesh of 1.63 million elements was selected for CFD analysis.

Table 3. The result of mesh independence study.

Number of Element	Calculated PCT
0.99 million	158.9℃
1.08 million	158.9℃
1.63 million	**159.3℃**
1.97 million	159.1℃
2.91 million	159.3℃
3.60 million	159.3℃

Since the emissivity of the inner wall of the basket was not specified in the experimental report, sensitivity analysis was performed. The sensitivity analysis range of the emissivity was carried out from 0.3 to 0.8. Here, 0.3 is the emissivity of 304L stainless steel, which is the basket material [6] and 0.8 is the emissivity of oxidized stainless steel [7].

The sensitivity analysis results are shown in Fig. 8. When the emissivity was increased from 0.3 to 0.8, the PCT dropped from 159.8 °C to 153.4 °C.
The inverse relationship between emissivity and the PCT is due to the nature of radiation. The basic radiant heat transfer rate equation is below:

$$q''_{rad} = \varepsilon\sigma(T_s^4 - T_{sur}^4)\,. \qquad (1)$$

where ε is the emissivity and σ is the Stefan-Boltzmann constant. According to Eq. (1), the higher the emissivity, the more active the radiative heat transfer. Therefore, the higher the emissivity of the inner wall of the basket, the lower the PCT. The emissivity to be used in the CFD analysis was selected based on the PCT measured in the experiment, and its value was 0.3215.

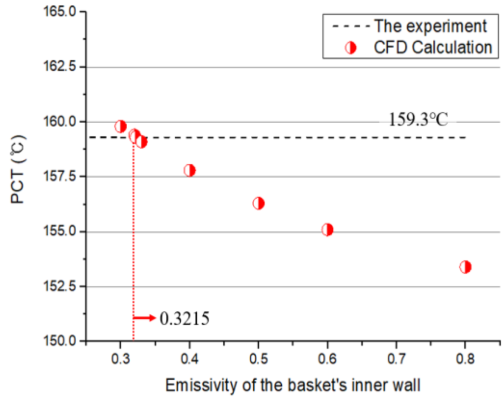

Fig. 8. Result of sensitivity analysis for emissivity.

The CFD analysis was performed using the input derived through the previous process. The object of this analysis was to evaluate thermal characteristics, especially the influence of each heat transfer mode. For the evaluation, the PCT according to the combination of heat transfer modes was calculated.

Table 4. Calculated PCT according to the combination of heat transfer modes.

Case	Combination of Heat Transfer Mode	PCT
1	Conduction + Convection + Radiation	159.3℃
2	Conduction + Convection	185.7℃
3	Conduction + Radiation	175.2℃
4	Conduction	294.7℃

And using the calculated PCTs, the thermal resistance for each heat transfer mode was evaluated. This evaluation was conducted based on three assumptions. The first assumption is that heat is transferred to the wall from the point where the PCT occurs, and the second assumption is that heat is transferred only in the radial direction. And the last assumption is that each thermal resistance is connected in parallel because conduction, convection, and radiation affect each other in the closed basket which has low heat source. Using these assumptions and the definition of thermal resistance, the following equations can be established:

$$Q = \frac{\Delta T}{R_{total}} = \frac{T_{peak} - T_{basket}}{(R_{cond}^{-1} + R_{conv}^{-1} + R_{rad}^{-1})^{-1}} = \frac{T_{peak} - T_{basket}}{(X+Y+Z)^{-1}}, \qquad (2)$$

$$R_{total} = \frac{\Delta T}{Q} \qquad (3)$$

where, Q is heat source. If the reciprocal of thermal resistance is X, Y, and Z, respectively, the following four equations can be established according to cases in Table 4.

Case 1: $X+Y+Z=\dfrac{Q}{T_{peak,1}-T_{basket}}$,

Case 2: $X+Y=\dfrac{Q}{T_{peak,2}-T_{basket}}$,

Case 3: $X+Z=\dfrac{Q}{T_{peak,3}-T_{basket}}$,

Case 4: $X=\dfrac{Q}{T_{peak,3}-T_{basket}}$. (4)

Representing the above four equations as a matrix,

$$\begin{pmatrix}1&1&1\\1&1&0\\1&0&1\\1&0&0\end{pmatrix}\begin{pmatrix}X\\Y\\Z\end{pmatrix}=\begin{pmatrix}\dfrac{Q}{T_{peak,1}-T_{basket}}\\\dfrac{Q}{T_{peak,2}-T_{basket}}\\\dfrac{Q}{T_{peak,3}-T_{basket}}\\\dfrac{Q}{T_{peak,4}-T_{basket}}\end{pmatrix}. \quad (5)$$

Since above Eq. (5) is an overdetermined system, the optimal solution for each heat transfer mode should be calculated. The results are summarized in Table 5.

Table 5. The result of thermal analysis for the basket with cylinder.

Heat transfer mode	Conduction	Convection	Radiation
Optimal thermal resistance	2.875°C/W	2.667°C/W	1.441°C/W
Q_{mode} / Q_{total}	24.55%	26.47%	48.98%

As a result of thermal analysis, it was evaluated that radiation has the greatest effect inside the storage basket, but convection and conduction also have a significant effect.

3. Two-Step Thermal Analysis for the Silo Facility

Thermal analysis of the silo facility was performed, and the analysis results were compared with the design criteria of the facility. For efficient thermal analysis, the basket geometry had to be simplified, and for this reason, a two-stop scheme was established. In the thermal analysis, CFD calculation was applied to the basket in which the fuel rod bundle was stored, unlike ch2, for a more realistic thermal analysis.

3.1 Two-Step Thermal Analysis Scheme

In the first of the two-step scheme for thermal analysis, the ETC correlation was derived using the CFD calculation result. As shown in Fig. 9-(a), the inner geometry of the basket is very complicate. Therefore, for efficient computational analysis, the basket was simplified to a homogeneous heating basket as shown in Fig. 9-(b).

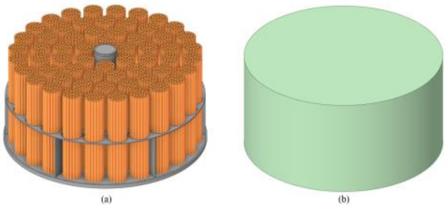

Fig.9. The storage basket with fuel bundles and the homogeneous heating basket.

And to predict the PCT in the homogeneous heating basket, ETC, which is a virtual thermal conductivity, was applied. In "Spent Nuclear Fuel Effective Thermal Conductivity Report [3]", the ETC was calculated using the PCT obtained through computational analysis and analytical solution for homogeneous heating solid. In the report, to calculate the PCT, CFD calculation was performed considering only conduction and radiation for 2D geometry. Based on the evaluation results of the basket in Ch.2, it was confirmed that convective heat transfer cannot be neglected. Accordingly, in this study, CFD calculations were performed considering radiation, convection, and conduction for 3D geometry. The ETC was calculated using this method, and as a result, 33 ETCs were obtained for boundary conditions (11 temperatures, 3 calorific values). And ETC correlation was derived by approximating these data in the form of equation below:

$$k_{eff}=f_1(q''')*T^3+f_2(q''')*T^2+f_3(q''')*T+f_4(q'''),$$
$$k_{eff}: ETC,$$
$$q''': Volumetric\ heat\ source\ of\ the\ basket,$$
$$T: Tempeature\ [K]. \quad (6)$$

In the second step, steady-state thermal analysis of the silo facility was performed. In the thermal analysis, homogeneous heating baskets with ETC correlation derived from the first step was applied. As boundary conditions, decay heat of the basket, natural convection heat transfer at the silo outer wall, radiation with ambient temperature, and insolation were considered.

3.2 Derivation of ETC Correlation Using CFD Calculation

The ETC was introduced to simplify the fuel storage basket into a homogeneous heating basket. Since the simplified geometry is an axisymmetric, effective thermal conductivity in the axial and radial directions is required. The axial ETC was calculated considering the volume ratio of the constituent materials of the basket. And radial ETC was calculated using CFD calculation and analytical solution, then expressed as a correlation between temperature and heat source.

To derive the ETC correlation, the CFD calculation result for the basket is needed. In addition, since calculations for various boundary conditions should be made, an input model for CFD calculation was derived and its validity was evaluated.

The geometry of the input model was generated by ANSYS SpaceClaim 2021 R2. Considering the symmetry of the basket design, an axisymmetric 1/6 basket was applied to the computational domain. In addition, the top and bottom plates of the basket were ignored, and the central lifting rod was also ignored.

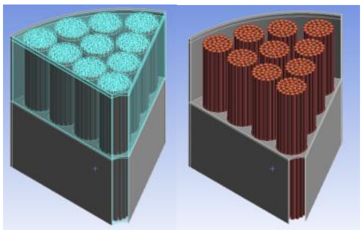

Fig.10. Geometry for the CFD Calculation.

The mesh was created using ANSYS Mesh 2021 R2. The FLUENT solver settings for thermal analysis are the same as in Table 2 above. Boundary conditions were set as shown in the Fig.10. The heat source of the basket was 360 W, and the isothermal condition applied to the outer wall of the basket was 115.2 °C.

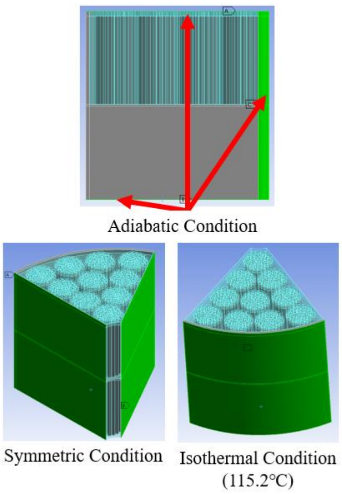

Fig. 11. Boundary condition for the CFD calculation.

The mesh independence study results are summarized in Table 6. In consideration of computational time, the mesh of 5.20 million elements was selected for the calculation.

Table 6. The result of mesh independence study.

Number of Element	Calculated PCT
5.20 million	**153.9°C**
5.83 million	153.9°C
7.34 million	154.0°C
8.50 million	154.1°C
12.18 million	154.3°C
12.48 million	154.3°C

To validate the input model, the storage basket thermal characteristic evaluation results were used. Since the evaluation was a CFD analysis of the basket in which the cylinder is stored, direct validation is not possible. Therefore, comparative analysis focused on identifying changes in heat transfer characteristics due to differences in the shape of cylinders and fuel bundles and evaluating the effects of the difference on PCT.

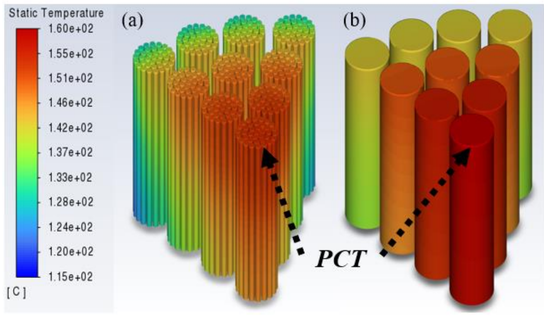

Fig. 12. Location of PCT.

Table 7. The calculated PCT between two CFD calculation.

	The Basket with Fuel Bundles	The Basket with Cylinders
PCT	153.9°C	159.3°C

According to the comparation results, the PCT is evaluated as low in the input model (basket with fuel bundles). The reason is the heat transfer area of the fuel rod bundle is about 5 times larger than that of the cylinder. In the basket, the most influential mode of heat transfer was radiation. And the larger heat transfer area means more active radiation. Consequently, the PCT is evaluated to be low in the fuel bundle with a large heat transfer area. As a result of comparative analysis, it was evaluated that the calculation result of this input model was sufficiently valid, and this input model was used to derive the ETC correlation.

In addition to the input model for CFD calculation, an analytical solution for simplified geometry is required for ETC calculation. And in previous studies [3], the following equation has been proposed.

$$k_{eff} = \frac{Q}{4\pi(T_{peak} - T_{basket})} \quad (6)$$

Eq. (6) was derived from the solution of the one-dimensional steady-state heat conduction problem of the heating cylinder. Therefore, it is not suitable for application to the storage basket, which is in the form of a heating annular cylinder. Therefore, the one-dimensional conduction heat transfer equation below should be solved again.

$$\frac{1}{r}\frac{d}{dr}\left(r\frac{dT}{dr}\right)+\frac{q'''}{k}=0 \quad (7)$$

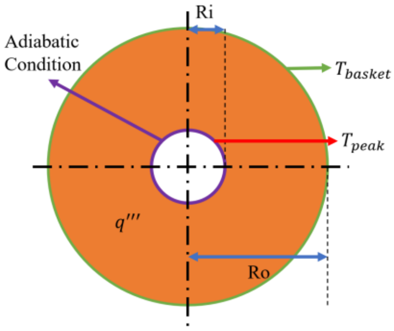

Fig. 13. Boundary Condition for heating annular cylinder.

By solving Equation (7) according to the given conditions in Fig. 13, the solution as shown in the following analytical solution (8) can be derived.

$$k_{eff}=\frac{q'''}{T_{peak}-T_{basket}}\left\{\frac{1}{4}(Ro^2-Ri^2)+\frac{1}{2}Ri^2(\ln Ri-\ln Ro)\right\},$$

where q''' is volumetric heat source. (8)

To calculate the PCT to be substituted in Eq. (8), CFD calculation was performed using the previously derived input model. The results are summarized in Table 8.

Table 8. The PCT calculated by CFD input model.

Basket Wall Temperature	Q (Heat source per basket, W)		
	260W	360W	560W
-15°C	19.0°C	29.2°C	38.9°C
15°C	49.5°C	59.8°C	69.6°C
30°C	64.7°C	74.8°C	84.5°C
60°C	94.7°C	104.8°C	114.4°C
90°C	124.7°C	134.7°C	144.2°C
120°C	154.7°C	164.5°C	173.8°C
150°C	184.5°C	194.1°C	203.2°C
180°C	214.0°C	223.5°C	232.5°C
220°C	252.7°C	262.1°C	270.8°C
260°C	290.9°C	299.9°C	308.4°C
300°C	328.6°C	337.2°C	345.3°C

A total of 33 ETCs were calculated using Eq. (8) and the calculated PCTs. And these data were curve-fitted with a third-order polynomial with respect to temperature. And the coefficients were expressed as a first-order polynomial for the heat source to derive a final correlation:

$$\begin{aligned} k_{eff} &= f_1(q''')*T^3+f_2(q''')*T^2+f_3(q''')*T+f_4(q'''),\\ f_1 &= -(5.81\times10^{-12})q'''+(1.80\times10^{-8}),\\ f_2 &= (5.39\times10^{-9})q'''-(1.66\times10^{-5}),\\ f_3 &= -(1.29\times10^{-6})q'''+(4.52\times10^{-3}),\\ f_4 &= (3.44\times10^{-4})q'''+(6.51\times10^{-1}). \end{aligned} \quad (9)$$

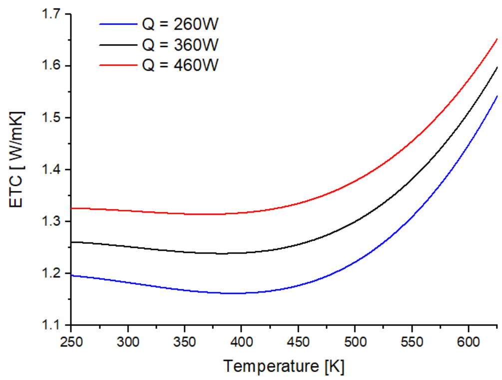

Fig. 14. Temperature - ETC along the Q.

To validate Eq. (9), PCT was calculated using the homogeneous heating basket model (ETC model) to which ETC calculated using the correlation above was applied. The results are summarized in Table 9. And it was compared with PCT (Table 8) calculated through input model.

Table 9. The PCT calculated by ETC model.

Basket Wall Temperature	Heat Source (W)		
	260W	360W	560W
-15°C	19.2°C	29.8°C	39.4°C
15°C	49.4°C	60.1°C	69.6°C
30°C	64.6°C	75.2°C	84.6°C
60°C	94.8°C	105.4°C	114.7°C
90°C	125.0°C	135.4°C	144.7°C
120°C	154.9°C	165.3°C	174.4°C
150°C	184.7°C	194.9°C	203.8°C
180°C	214.1°C	224.2°C	233.0°C
220°C	252.9°C	262.6°C	271.2°C
260°C	291.1°C	300.5°C	308.9°C
300°C	328.8°C	337.8°C	346.0°C

Table 10. PCT difference (CFD input model vs. ETC model).

Basket Wall Temperature	Heat Source		
	260W	360W	560W
-15℃	0.2℃	0.6℃	0.5℃
15℃	-0.1℃	0.3℃	0℃
30℃	-0.1℃	0.4℃	0.1℃
60℃	0.1℃	0.6℃	0.3℃
90℃	0.3℃	0.7℃	0.5℃
120℃	0.2℃	0.8℃	0.6℃
150℃	0.2℃	0.8℃	0.6℃
180℃	0.1℃	0.7℃	0.5℃
220℃	0.2℃	0.5℃	0.4℃
260℃	0.2℃	0.6℃	0.5℃
300℃	0.2℃	0.6℃	0.7℃

Referring to Table 10, the PCT calculated by the ETC model is slightly overestimated compared to PCT from the CFD input model. However, since the degree of overestimation is less than 1℃, it was evaluated that the ETC model predicts PCT well. Therefore, the derived ETC correlation is suitable for thermal analysis of the silo facility.

3.3 Thermal Analysis for the Silo Facility

Considering design of the silo, geometry is generated with 1/4 axisymmetric. ANSYS SpaceClaim 2021 R2 was used for geometry generation.

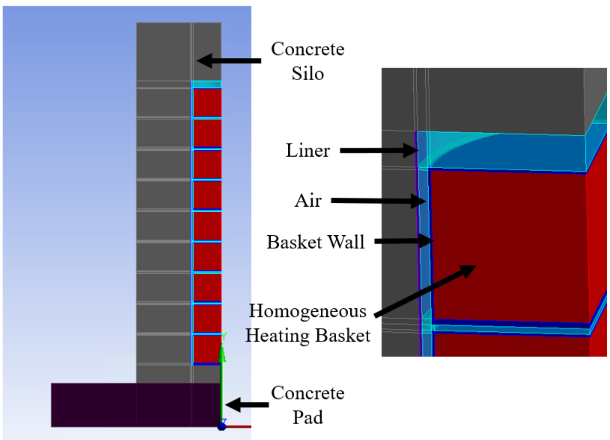

Fig. 15. Silo geometry for the thermal analysis.

The mesh was created using ANSYS Mesh 2021 R2. The FLUENT solver setup is summarized in Table 11. Boundary conditions were set as shown in Table 12 below. Natural convection conditions and radiation from ambient temperature were applied to the outer wall of the silo. For the ambient temperature, the average annual maximum temperature of Korea was applied. In the case of insolation, the average daily insolation was applied considering the thermal inertia of the silo. The decay heat of the basket was applied to 364.8W. All boundary conditions were set conservatively.

Table 11. FLUENT solver setup.

Viscous Model		Laminar Model
Radiation Model		DO model
Density Model		Constant
Pressure – Velocity Coupling		SIMPLE
Spatial Discretization	Gradient	Least Squares Cell Based
	Pressure	Standard
	Momentum	2nd Order Upwind
	Energy	2nd Order Upwind
	DO	2nd Order Upwind

Table 12. Boundary condition for thermal analysis.

Ambient Temperature		22℃
Vertical Outer Wall of Silo	Natural Convection	$h_v = (\frac{k_{air}}{H}) \times 0.59(\Pr \cdot Gr)^{1/4}$ [7]
	Isolation	194 W/m²
Horizontal Outer Wall of Silo	Natural Convection	$h_h = (\frac{k_{air}}{D}) \times 0.54(\Pr \cdot Gr)^{1/4}$ [7]
	Isolation	388 W/m²
h_v : *Convection heat transfer coefficient in the vertical surface* $[W/m^2K]$ h_h : *Convection heat transfer coefficient in the horizontal surface* $[W/m^2K]$ k_{air} : *Thermal conductivity of air* $[W/mK]$ H: *Height of the silo* $[m]$ D: *Diameter of the silo* $[m]$ $\Pr$: *Number of Prandtl* Gr : *Number of Grashof*		
Symmetric Condition		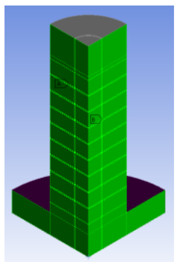
Adiabatic Condition		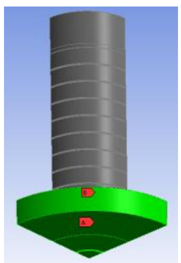

The mesh independence study results are summarized in Table 3 below, and the mesh of 1.71 million elements was selected for CFD analysis.

Table 13. The result of mesh independence study.

Number of Element	Calculated PCT
1.71 million	140.2℃
3.41 million	140.4℃
5.05 million	140.5℃
22.9 million	140.4℃

Steady-state thermal analysis of the silo facility was performed using the derived input. Analysis results and design criteria are summarized in Table 14. As for design criteria, ACI-349 [8] for concrete, ASME [9] for liner and basket shell, and SAR [1] for cladding were referenced.

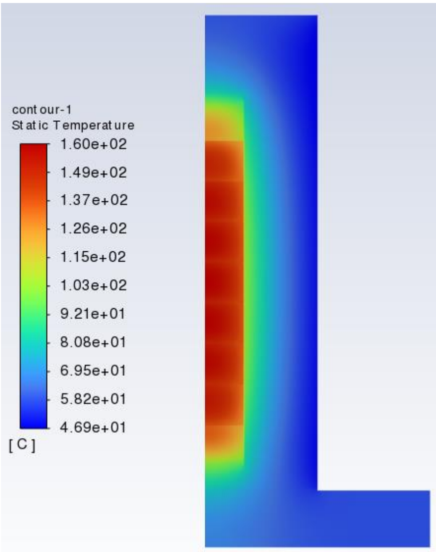

Fig. 16. Temperature distribution in steady-state analysis.

Table 14. Design criteria vs. calculated temperature.

	Design Criteria	Calculated Maximum Temperature
Concrete	93℃	101℃
Liner (SA516)	371℃	102.2℃
Basket (SA240-304L)	427℃	153.6℃
Cladding	180℃	**160.0℃**

As a result of thermal analysis of the silo facility, it was evaluated that the cladding, basket, and liner had sufficient margins for the design criteria. However, it was evaluated that the concrete did not satisfy the design criteria. Therefore, the subject of future research is to analyze the validity of boundary conditions and evaluate their impact on each component.

4. Conclusions

In this study, the thermal analysis of CANDU spent fuel storage silo was performed using a CFD code. Prior to the thermal analysis, the thermal characteristics of the fuel storage basket were evaluated, and it was confirmed that radiative heat transfer had the greatest influence. And a two-step scheme was derived to perform the thermal analysis of the silo facility. The first step was to derive the ETC correlation for the simplification of the fuel storage basket. CFD code was used for ETC calculation. The model to which ETC correlation was applied predicted PCT well. In the second step, the thermal analysis of the silo facility with the simplified basket was performed. The boundary conditions for the analysis were set conservatively. As a result of the analysis, the cladding, basket, and liner all satisfied the design criteria, but the concrete did not.

In future research, evaluation of whether the boundary conditions set for thermal analysis of silo facilities are appropriate and thermal analysis using transient CFD calculation and transient 1D code are planned.

ACKNOWLEDGEMENT

This research was supported by the Central Research Institute, Korea Hydro & Nuclear Power Co., Ltd., funded by the Korea Institute of Energy Technology Evaluation and Planning.

REFERENCES

[1] KEPCO, Project Safety Analysis Report Spent Fuel Dry Storage Wolsong Nuclear Power Plant Unit 1, 1991.
[2] TRW Environmental Safety Systems Inc, Spent Nuclear Fuel Effective Thermal Conductivity Report, U.S. Department of Energy, pp.80-81, 1996.
[3] AECL Whiteshell Lab, Storage Basket Heat Transfer Assessment of the MACSTOR/KN-400 Storage Module, Technical Document, 2002.
[4] D.G. Lee. et al., An Assessment of Temperature History on Concrete Silo Dry Storage System for CANDU Spent Fuel, Annals of Nuclear Energy, 2016.
[5] U.S.NRC, NUREG-2152, Computational Fluid Dynamics Best Practice Guidelines for Dry Cask Applications.
[6] H. Y. Nam, K. Y. Lee, J. M. Kim, S. K. Chio, J. H. Park, I. K. Choi, Experimental study on the emissivity of stainless steel, Proceedings of the Korean Nuclear Society spring meeting, 2001.
[7] F. P. Incropera et.al., Principles of Heat and Mass Transfer, 8th Edition, Wiley, pp.539~540,902-903, 2019.
[8] ACI Committee, ACI CODE-349-13: Code Requirements for Nuclear Safety-Related Concrete Structures and Commentary, 2014.
[9] ASME Section III Division 1, 2017.